


Adaptive control to actively damp bistabilities in highly interrupted turning processes using a hardware-in-the-loop simulator

Journal of Vibration and Control
2021, Vol. 0(0) 1–10
© The Author(s) 2021
Article reuse guidelines:
sagepub.com/journals-permissions
DOI: 10.1177/10775463211057968
journals.sagepub.com/home/jvc


Govind N. Sahu¹ , Mohit Law¹  and Pankaj Wahi²

Abstract

Interruptions in turning make the process forces non-smooth and nonlinear. Smooth nonlinear cutting forces result in the process of being stable for small perturbations and unstable for larger ones. Re-entry after interruptions acts as perturbations making the process exhibit bistabilities. Stability for such processes is characterized by Hopf bifurcations resulting in lobes and period-doubling bifurcations resulting in narrow unstable lenses. Interrupted turning remains an important technological problem, and since experimentation to investigate and mitigate instabilities are difficult, this paper instead emulates these phenomena on a controlled hardware-in-the-loop simulator. Emulated cutting on the simulator confirms that bistabilities persist with lobes and lenses. Cutting in bistable regimes should be avoided due to conditional stability. Hence, we demonstrate the use of active damping to stabilize cutting with interruptions/perturbations. To stabilize cutting with small/large perturbations, we successfully implement an adaptive gain tuning scheme that adapts the gain to the level of interruption/perturbation. To facilitate real-time detection of instabilities and their control, we characterize the efficacy of the updating scheme for its dependence on the time required to update the gain and for its dependence on the levels of gain increments. We observe that higher gain increments with shorter updating times result in the process being stabilized quicker. Such results are instructive for active damping of real processes exhibiting conditional instabilities prone to perturbations.

Keywords

Interrupted turning, bistable, chatter, hardware-in-the-loop simulator, active damping, adaptive control

1. Introduction

Turning of gear teeth or shafts with grooves and keyways are examples of processes that are interrupted. When the ratio of the time spent in cutting to the spindle period is small, these processes are deemed highly interrupted. If, during such interrupted processes, the tool and/or the workpiece is flexible, the intermittent excitations may result in self-excited unstable vibrations due to the regenerative effect, that is, due to the Hopf bifurcation. In addition, in highly interrupted turning, sometimes there is an additional loss of stability due to period-doubling bifurcations resulting in stability lenses (Corpus and Endres, 2004; Stépán et al., 2005; Szalai and Stépán, 2006). Furthermore, the interruptions make the cutting forces non-smooth (Zanka et al., 2010), and nonlinear (Chen et al., 2015; Corpus and Endres, 2004; Stépán et al., 2005; Szalai and Stépán, 2006). The smooth cutting force nonlinearities make the process unstable for large perturbations, while for small ones, it remains stable, thus forming a bistable region

(Kalmar-Nagy et al., 1999; Shi and Tobias, 1984). Since interruptions are perturbations, it is likely that bistabilities may co-occur with Hopf and period-doubling bifurcations. Mitigating instabilities in interrupted turning remains an important and unaddressed technological problem (Seguy et al., 2014; Urbikain et al., 2014). Accordingly, the main aim of this paper is to investigate and mitigate bistable behaviour co-occurring with bifurcations in highly interrupted machining.

¹Machine Tool Dynamics Laboratory, Department of Mechanical Engineering, Indian Institute of Technology Kanpur, Kanpur, India

²Department of Mechanical Engineering, Indian Institute of Technology Kanpur, Kanpur, India

Received: 14 April 2021; accepted: 19 October 2021

Corresponding author:

Mohit Law, Machine Tool Dynamics Laboratory, Department of Mechanical Engineering, Indian Institute of Technology Kanpur, Kanpur 208016, India.
Email: mlaw@iitk.ac.in

Stability of interrupted cutting has been studied for turning and for low radial immersion milling processes. Robust numerical methods using the semi-discretization technique (SDM) (Insperger and Stépán, 2004) and/or closed-form analytical formulae have shown being capable of predicting Hopf and flip bifurcations in interrupted cutting processes (Davies et al., 2002; Szalai and Stépán, 2006). Models can predict bifurcations, and stability lenses in milling have been shown to exist experimentally (Bayly et al., 2003; Corpus and Endres, 2004; Davies et al., 2002). Even though stability of interrupted turning processes has been theoretically examined by many (Corpus and Endres, 2004; Stépán et al., 2005; Szalai and Stépán, 2006), and experimentally by some (Seguy et al., 2014; Urbikain et al., 2014), conclusive experimental proof for bistabilities co-occurring with lenses in interrupted turning remains elusive. Providing such proof is one of the small contributions of the current work.

Since cutting in bistable regions should be avoided, analytical models established for finding the location and size of these bistable regions are useful (Dombovari et al., 2008; Molnar et al., 2019). If cutting is still desired to be carried out at parameters that lie within the bistable region, active damping schemes may help stabilize an otherwise unstable process. However, for processes that are nonlinear, bistabilities persist with traditional implementations of active damping schemes (Sahu et al., 2021). To stabilize cutting with small/large perturbations in the presence of process nonlinearities, the use of other robust and/or adaptive control schemes may be necessary which has been demonstrated in the current paper.

Robust active control of machine tool vibrations has been shown to be effective to mitigate instabilities due to changing and nonlinear dynamics (Abele et al., 2016; Zaeh et al., 2017). Adaptive control has also shown to be effective to mitigate chatter instabilities (Claesson and Håkansson, 1998; Fallah and Moetakef-Imani, 2019; Kleinwort et al., 2018). However, since these previous uses of robust and/or adaptive control schemes required dynamical models of the machine tool and the process, they are less suited for industrial implementation, which prefers the simple to implement non-model based schemes (Chung et al., 1997; Cowley and Boyle, 1969; Mancisidor et al., 2015b; Munoa et al., 2013). Even though different model and non-model based active damping solutions have been effective, control techniques to eliminate bistabilities in the presence of interruptions/perturbations remain unexplored and will be addressed herein.

Since characterizing instabilities to mitigate them on real machines involves several (in)stability experiments that are difficult and those which could potentially damage the machine tool system, we prefer to emulate these phenomena on a hardware-in-the-loop (HiL) simulator. The main goal of the present HiL simulator is to emulate chatter in the presence of cutting process-nonlinearities and devise strategies to mitigate it. It is not the aim of emulations on the

HiL simulator to be compared with the real cutting processes, but instead to guide cutting parameter selection and detection and suppression of chatter during real cutting. HiL simulators for emulating cutting process stability consist of a hardware layer approximating a flexible workpiece and an actuator that emulates real-time regenerative cutting forces estimated in the software layer. Previous uses of HiL simulators have proven useful to emulate stability in turning and to test various active damping control strategies (Ganguli et al., 2005; Mancisidor et al., 2015a; Sahu et al., 2020; Stepan et al., 2019). Period-doubling bifurcations occurring in low radial immersion milling have also been successfully emulated on a HiL simulator (Ganguli et al., 2006), as have bistabilities with different nonlinear force characteristics (Sahu et al., 2021). Though period-doubling bifurcations and bistabilities have previously been separately emulated on HiL simulators, their potential co-occurrence in highly interrupted turning remains unexplored – something this paper aims to address. Furthermore, to stabilize cutting with small/large perturbations in the presence of process nonlinearities, we implement a non-model based adaptive controller using velocity feedback, which we prefer, for it has been shown to be better than acceleration, delayed acceleration, and/or delayed displacement feedback (Mancisidor et al., 2015b; Munoa et al., 2013; Sahu et al., 2020).

The remainder of the paper is structured as follows: in Section 2, the mechanical model of interrupted turning with nonlinear force characteristics is described. We also discuss the linearization of the resulting nonlinear delay differential equations (DDE) about the mean chip thickness. This section also discusses finding the globally unstable limit using the SDM (Insperger and Stépán, 2004), and finding the globally stable limit using analytical closed-form formulae (Molnar et al., 2019). The HiL simulator is described in Section 3. Section 4 presents emulated results on the HiL simulator and compares them with model predictions, and we show how bistabilities persist with lenses. Section 5 presents an adaptive control technique to eliminate bistable behaviour in the case of highly interrupted turning processes. Main conclusions follow these discussions.

2. Mechanical model of interrupted turning with cutting process nonlinearities

The mechanical model of an interrupted turning process is shown in Figure 1. We follow the model presented in Szalai and Stépán, (2006). We limit our investigations herein only to the case of a single interruption. For simplicity, the tool is assumed to be rigid, and the workpiece to be flexible in the feed direction. This makes it akin to a single degree of freedom system.

From Figure 1, the governing equation of motion is

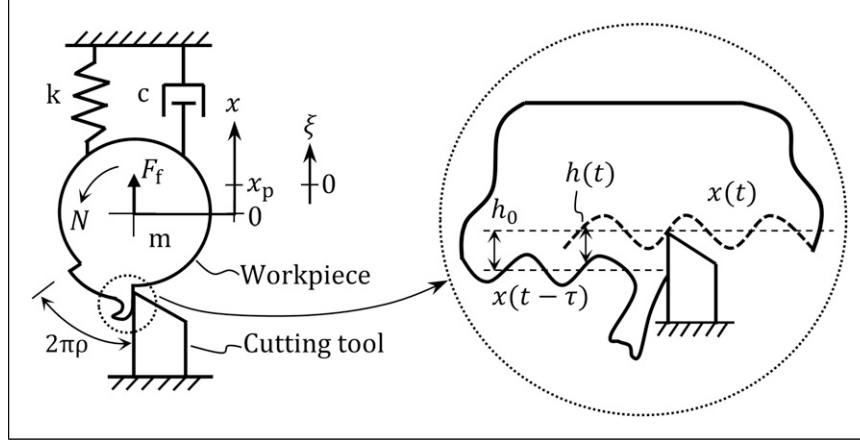


Figure 1. Mechanical model of simple interrupted turning process.

$$\ddot{x}(t) + 2\zeta\omega_n\dot{x}(t) + \omega_n^2x(t) = \frac{F_f(t)}{m} \quad (1)$$

wherein m , ζ and ω_n are the modal mass (kg), the damping ratio and the natural frequency (rad/s) of the workpiece, respectively. The cutting force, $F_f(t)$, is described by the product of a cutting force coefficient, depth of cut (b), and the total chip thickness ($h(t)$), that is, $F_f(t) = bf(t)$, wherein $f(t)$ is assumed to be nonlinearly dependent on the chip thickness as (Corpus and Endres, 2004; Kalmár-Nagy et al., 1999; Kienzle, 1952)

$$f(t) = K_f h(t)^v, \quad (2)$$

wherein K_f and v are empirically determined coefficients.

For the case of a single interruption in a revolution, the angle of the cutting zone is $2\pi\rho$, wherein ρ is cutting ratio, that is, the ratio of the time spent in the cutting zone to the spindle period. To track the instantaneous cutting force becoming zero in the non-cutting zone, a screening function, $g(\theta(t))$ is introduced in $F_f(t)$ as

$$F_f(t) = g(\theta(t)) bf(t), \quad (3)$$

wherein $g(\theta(t))$ is

$$g(\theta(t)) = \begin{cases} 1 & 0 \leq \theta \leq 2\pi\rho \\ 0 & 2\pi\rho \leq \theta \leq 2\pi(1-\rho). \end{cases} \quad (4)$$

The instantaneous angular position ($\theta(t)$) of the workpiece with respect to time can be tracked as: $\theta(t) = (2\pi N/60)t + 2\pi/N_p$, wherein N is the spindle speed in rpm and N_p is number of interruptions, which is one in the present case.

Since the cutting forces excite the workpiece that is flexible, vibration marks are imprinted on the workpiece surface as a wavy profile. As the workpiece rotates, the tool encounters the wavy surface generated in the earlier revolution. This regenerative phenomenon is shown schematically in Figure 1. Due to the interactions, the total chip

thickness depends on the specified chip thickness, h_0 , and the vibration of the current ($x(t)$) and previous revolution(s) ($x(t-\tau)$), and can be calculated as: $h(t) = h_0 - x(t) + x(t-\tau)$, wherein $\tau = 60/N$ is the period of one revolution in seconds. If vibrations are large, the tool may jump out of the cut. The loss of contact between the tool and the workpiece results in the force becoming zero, that is, $F_f(t) = 0$ when $h(t) \leq 0$. This self-interruption in the cutting process may occur along with the inherent parametric interruption, and further leads to multiple regenerative effects and saturation of chatter amplitudes (Tlustý and Ismail, 1981).

We assume that the workpiece vibrates with a form of $x(t) = x_p(t) + \zeta(t)$, wherein $x_p(t)$ is the amplitude of vibration in the chatter free condition and $\zeta(t)$ is the vibrational amplitude of the workpiece after any perturbation from $x_p(t)$. Due to τ -periodicity, it follows that $x_p(t) = x_p(t+\tau)$. Substituting this form of $x(t)$ in equation (1) and using the nonlinear form of the force in equation (2), the resulting equation of motion becomes a nonlinear DDE

$$\begin{aligned} \ddot{x}_p(t) + 2\zeta\omega_n\dot{x}_p(t) + \omega_n^2x_p(t) + \ddot{\zeta}(t) + 2\zeta\omega_n\dot{\zeta}(t) \\ + \omega_n^2\zeta(t) = \frac{K_f b}{m} g(\theta(t))(h_0 + \zeta(t-\tau) - \zeta(t))^v. \end{aligned} \quad (5)$$

The nonlinear force in this DDE is first linearized using a Taylor series up to first order approximation about the mean chip thickness (Sahu et al., 2021), and the linearized form of equation (5) in ζ becomes

$$\ddot{\zeta}(t) + 2\zeta\omega_n\dot{\zeta}(t) + \omega_n^2\zeta(t) = \frac{b}{m} q(t)(\zeta(t-\tau) - \zeta(t)) \quad (6)$$

wherein, $q(t) = g(\theta(t))K_f v h_0^{v-1}$.

Equation (6) is solved for stability using the semi-discretization method (SDM) (Inspurger and Stépán, 2004), in which we first transform the linearized DDE (equation (6)) to its first order form as given below

$$\dot{\xi}(t) = \mathbf{A}(t)\xi(t) + \mathbf{B}(t)\xi(t - \tau), \quad (7)$$

where in $\mathbf{A}(t) = \begin{bmatrix} 0 & 1 \\ -\left(\omega_n^2 + \frac{q(t)b}{m}\right) & -2\zeta\omega_n \end{bmatrix}$, $\mathbf{B}(t) = \begin{bmatrix} 0 & 0 \\ \frac{q(t)b}{m} & 0 \end{bmatrix}$. In SDM, the stability of the system is

obtained by estimating the eigenvalue of the resulting transition matrix from equation (7). The critical stability limit of the system is obtained when the modulus of eigenvalue is unity. Stability is characterized by probing different depths of cut for different spindle speeds under consideration. The stability boundaries thus obtained correspond to the global unstable limits and include both lobes and lenses.

Global stable limits are obtained using closed-form formulae (Molnar et al., 2019) in which, if the global unstable limit is b_{lim} and if the size of the bistable region is R_{bist} , then the global stable limit (b_{bist}) of the bistable region can be estimated as

$$b_{bist} = (1 - R_{bist})b_{lim}. \quad (8)$$

The size of the bistable region is (Molnar et al., 2019)

$$R_{bist} = 1 - \frac{\sqrt{\pi} \Gamma(v+2)}{2^{v+1} \Gamma(v+\frac{1}{2})}, \quad (9)$$

wherein Γ is the Euler gamma function, and v is the same cutting exponent as in equation (2).

Having described the mechanical model for interrupted turning and having discussed methods to solve for the globally (un)stable limits, we now discuss the use of the HiL simulator to emulate the same.

3. Hardware-in-the-loop (HiL) simulator

The HiL simulator contains a hardware and a software layer as shown in Figure 2. These layers interact with each other in a closed-loop sense to emulate the physics of cutting tool-workpiece interactions. The HiL simulator platform used herein is the same as reported in

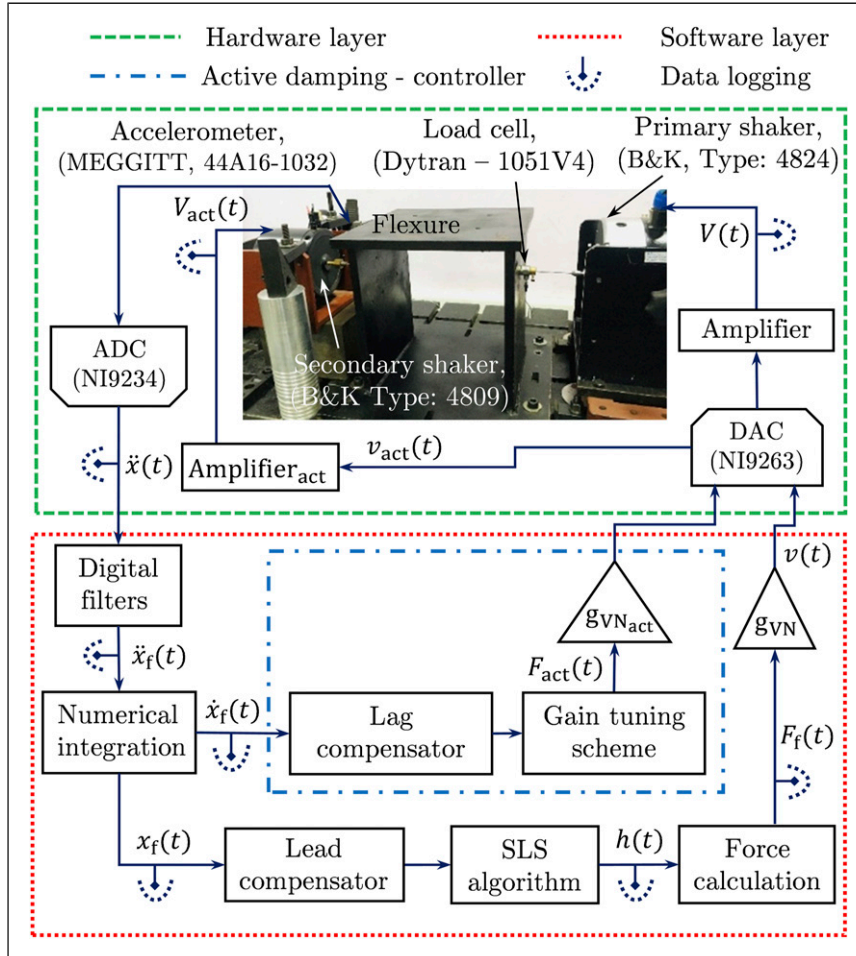


Figure 2. Block diagram of the hardware-in-the-loop simulator for turning process.

Sahu et al. (2020, 2021). Hence, for details, the interested reader is directed there.

The hardware layer includes two shakers. The primary shaker has a force capacity of 100N, and its power amplifier is operated in the DC voltage mode. The secondary shaker has a force capacity of 45N, and its power amplifier is operated in the AC voltage mode. The primary shaker applies a simulated regenerative cutting force on the flexure, and the secondary shaker applies an active damping force to the same flexure (see Figure 2). Both shakers are fixed on a rigid table and are connected to the flexure via stingers. The length of the stingers and boundary conditions of the shaker are chosen such that the shaker's dynamics have minimal influence on the flexure. Shakers are also operated such that they do not saturate in stroke and/or current. The flexure is designed and observed to act like a single degree of freedom system emulating a flexible workpiece. The modal parameters of the flexure are identified to be $m = 16.57$ kg, $k = 9.1737 \times 10^6$ N/m, $\zeta = 0.29$ % and $f_n = 118.4$ Hz. Force-voltage characteristics of both shakers were evaluated, and the primary shaker was observed to have a gain, g_{VN} , of 0.06 V/N and the secondary, a gain, g_{VNact} , of 0.028 V/N. Frequency-phase characteristics of the shakers were used to estimate a delay attributable to the shaker(s).

The software layer is written in NI LabVIEW and includes data acquisition and digital filtering of acquired acceleration signals. The software layer also calculates the total chip thickness using a forward Euler based real-time numerical integration scheme in which displacements are obtained from accelerations. Regenerative forces are calculated in the software layer from the estimated chip thickness, and active damping forces are estimated from velocities. The software layer runs at the rate of 5kHz, and it includes real-time display and data logging for post-processing of acquired data. Signal processing in the software layer also contributes to a delay – which along with the delay due to the hardware layer, are compensated as detailed in Sahu et al. (2020, 2021). Multiple regenerative effects and basic nonlinearities of tool jumping out of cut are incorporated in the software layer using an efficient surface location storage – details of which are available in Sahu et al. (2021). The calculated real-time regenerative cutting force ($F_f(t)$) and active damping force ($F_{act}(t)$) are converted to voltage signals $v(t)$ and $v_{act}(t)$, respectively, and supplied to their respective power amplifiers using a digital-to-analogue device.

4. Emulating bistability and lenses

This section describes the experimentally emulated behaviour on the HiL simulator. For the force model, we assume a power of $\nu = 0.41$ (Kalmar-Nagy et al., 1999) and take the coefficient to be $K_f = 2 \times 10^6$ N/m^{1+ ν} that corresponds to cutting a typical hardened steel. We emulate cutting behaviour for a mean chip thickness of $h_0 = 10$ μ m

and check for bistabilities in lobes and lenses for a cutting ratio of $\rho = 0.2$.

The procedure to experimentally identify the globally unstable limit is as follows: first, at a specified depth of cut (b), spindle speed (N) and static chip thickness (h_0), we perturb the flexure with a static load proportional to the static chip thickness. If in response to this perturbation, the measured displacement signal decays, the system is said to be stable. We then sequentially increase the depth of cut in steps of 5 μ m. If the amplitude of displacement signal increases such that it saturates at finite amplitudes and if the calculated cutting forces in the cutting zone become zero at certain time instants due to the tool jumping out of the cut phenomenon, then the system is said to be unstable. The corresponding depth of cut, spindle speed, and chatter frequency is recorded as the globally unstable limit. For experimentally identifying the globally stable limit, the depth of cut is sequentially decreased from the globally unstable point in the same steps taken to find the globally unstable limit. This results in a decrease in displacement response (chatter amplitude). For a specified spindle speed and mean chip thickness, the globally stable limit is considered at the last depth of cut corresponding to loss of contact in the cutting zone. The standard *if* and *else* condition is implemented in the software layer for easy identification of globally unstable and stable points. Using this technique, experiments are conducted for every spindle speed under consideration, and the resulting experimentally emulated stability is overlaid over theoretical predictions in Figure 3. Theoretical globally unstable limits are obtained by solving equation (7), and globally stable limits are obtained using equations (8) and (9).

As is evident in Figure 3, experimentally emulated bi-stable behaviour agrees with theoretical predictions. Also evident is that even within the lenses where there is an additional loss of stability in the speed range between 4700 r/min–4900 r/min, bistability persists. This suggests that parametric interruption in the cutting process does not modify the width of bistable regions. To probe the nature of bifurcations, the flexure's measured displacement overlaid with once-per-revolution sampled data, Poincare sections, and the power spectrum of the displacement signals corresponding to the points A, B and C (marked in Figure 3) are shown in Figure 4. The three points correspond to a constant depth of cut, $b = 0.6$ mm, and the spindle speeds are $A \rightarrow 4050$ r/min, $B \rightarrow 4700$ r/min and $C \rightarrow 4770$ r/min. 'A' lies above the traditional stability boundary, 'B' lies below the boundary, and 'C' lies within the lens.

As is evident from Figure 4, since point 'A' lies above the conventional stability boundary, its response suggests unstable behaviour, and the once-per-revolution sampled data shows a quasiperiodic behaviour – which is characteristic of a Hopf bifurcation. Poincare section of point 'A' also suggests unstable behaviour and forms a limit cycle due to saturation of chatter amplitude resulting from the tool out

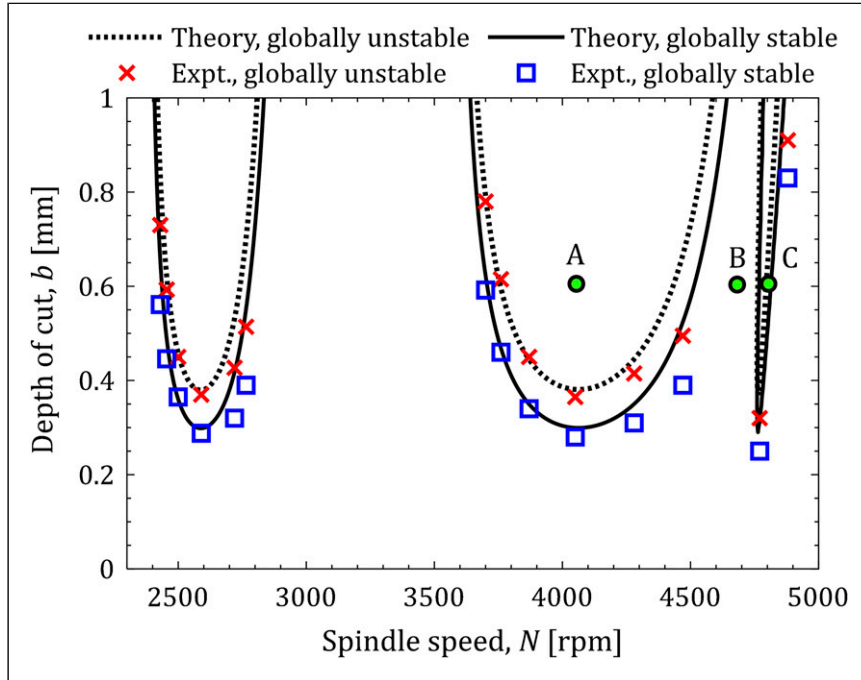


Figure 3. Comparison of theoretically predicted and emulated stability on the HiL simulator.

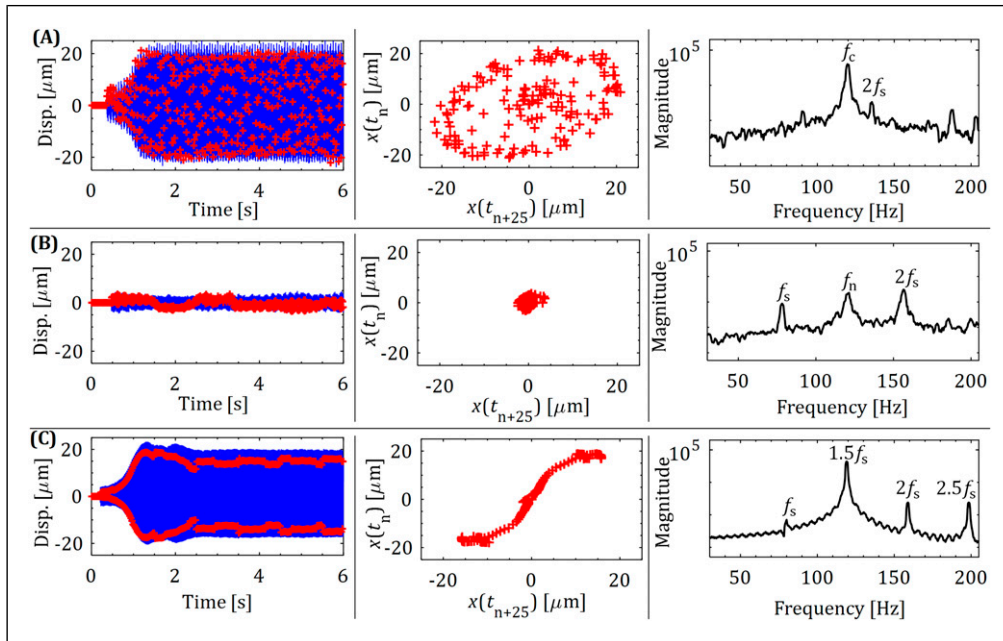


Figure 4. Measured displacement signal (blue line) overlaid with data sampled at once-per-revolution ('+' symbol) – shown in the first column; Poincare sections of the once-per-revolution data – shown in the second column; Power spectrum of measured displacement signal – shown in the third column. For cutting parameters for points 'A', 'B', and 'C' please refer to Figure 3.

of cut phenomenon. The power spectrum of the displacement signal shows the dominant chatter frequency (f_c) along with the harmonics of the virtual spindle frequency ($f_s = nN/60$, where $n = 1, 2, 3, \dots$), which are characteristics of unstable Hopf bifurcations. Point 'B'

corresponds to a stable cutting case, and since the motion of the flexure is periodic, the flexure oscillates at the virtual spindle frequency and its harmonics (f_s and $2f_s$), and hence, an approximately straight line is observed when the displacement signal is sampled once-per-revolution.

For emulated cutting at point ‘C’, since ‘C’ lies within the lens, its response suggests unstable behaviour, and the once-per-revolution sampled data shows that the motion is unstable with its dominant unstable frequency being the sub-harmonic of the virtual spindle frequency ($1.5f_s$ and $2.5f_s$). Hence, the once-per-revolution sampled data appear as a pair of points offset from each other in the vertical direction – thus confirming that this is a case of flip bifurcation.

Such emulations on the HiL simulator are useful to study chatter in a non-destructive manner on a controlled platform. Emulated behaviour is not meant to be compared to real cutting processes, but is meant to guide cutting parameter selection, and to detect and mitigate chatter during real cutting.

5. Adaptive active damping of bistabilities

Since bistabilities persist with lobes and lenses in interrupted turning, the process will be conditionally stable if cutting were to be conducted in the bistable regions. As has been already demonstrated elsewhere (Sahu et al., 2021), it is possible to actively damp instabilities and improve the globally stable limit. However, since the process remains nonlinear, bistabilities will persist even in the improved boundaries. Hence, to stabilize cutting in the bistable region in the presence of small/large perturbations, we propose an adaptive gain tuning scheme as outlined in Figure 5. The aim of this scheme is to detect if the process is unstable under perturbations and update the gain appropriately until the process stabilizes even with large perturbations.

The adaptive gain updating procedure works as follows: at first, for the given cutting parameters, we determine if the cut is stable or not. Stability is determined based on the frequency content within the measured displacements of the flexure. The frequency spectra of a stable cut contain only the spindle frequency (f_s) or its main harmonics. An unstable cut is classified as that in which the dominant frequency ($f_{A_{max}}$) is not the spindle frequency (f_s) or any of its main harmonics, that is, $f_{A_{max}} \neq n f_s$, wherein $n \in 1 : 10$. To account for noise in signals, valid frequency content is treated as that with magnitudes greater than $0.1 \mu\text{m}$ – which is the noise floor. If instability is detected, since the gain is initialized to a user preset value, and if with this gain the force applied by the actuator deems the cut stable, adaptive tuning is not necessary. However, if, even with the force applied with the initialized gain, the cut is still unstable, the gain is updated in increments of dK until such time as the cut becomes stable and/or the actuator nears its force capacity. Since we prefer the use of a direct velocity feedback control scheme, in which the force applied by the active damper is proportional to the gain and to the measured velocity of vibration, the maximum gain allowable is limited by the actuator’s force capacity. To ensure that the actuator does not saturate in force, we limit the saturation gain to $K_{sat} = 200 \text{ Ns/m}$, which is well below the identified maximum control gain of $\sim 300 \text{ Ns/m}$.

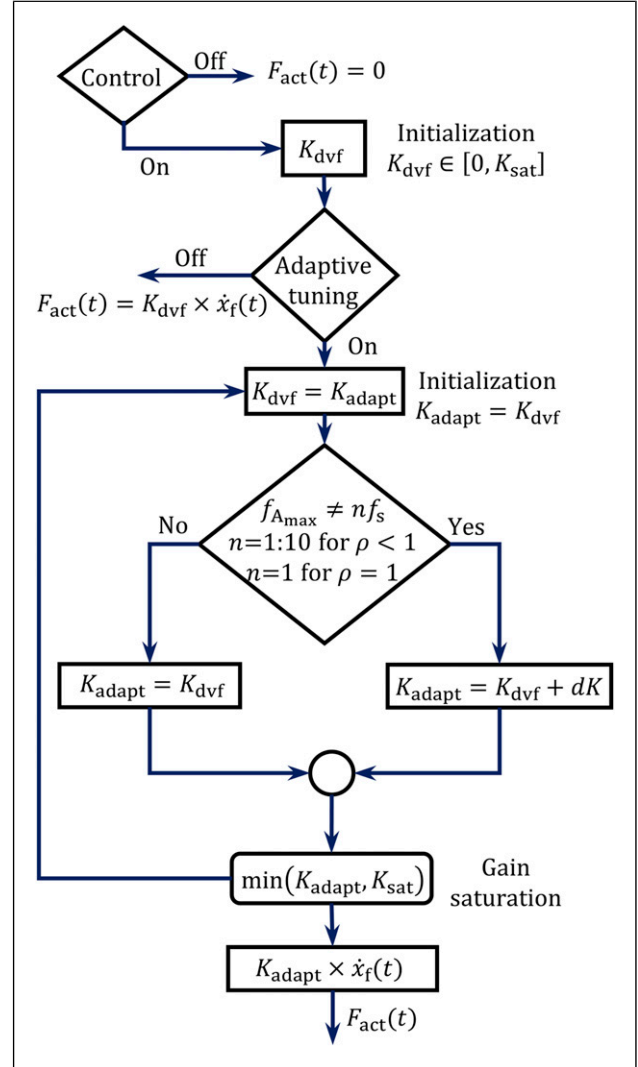


Figure 5. Flowchart of the adaptive control scheme.

Since the proposed adaptive gain tuning scheme is meant to work in real-time, we first characterize the efficacy of the method for its dependence on the time required to update the gain as well as to characterize the scheme for its dependence on the levels of gain increments, dK . Since real-time estimation of the frequency content of the displacement signal is necessary, we use the inbuilt Fast Fourier Transform (FFT) function within LabVIEW to estimate the frequency content. To account for the main harmonics of the excitation frequency, we consider 750 data points in a sample. The FFT estimate from this sample takes 0.15s. We call this the DAQ time. Since instabilities can fully develop within this DAQ time, and since instabilities are destructive, we investigate the performance of the adaptive scheme with four different levels of gain updating time. These are taken to be 25, 50, 75 and 100% of the DAQ time. For each of these configurations, we also explore the role played by the gain increment by considering four different values of $dK \in [1, 2, 10, 200] \text{ Ns/m}$.

Before testing the adaptive gain tuning method's efficacy in stabilizing cutting in the bistable zone in the presence of perturbations, we characterized its dependence on the gain increment level and the time required to update the gain. These experiments were conducted at a fixed operating point with a depth of cut of $b = 0.8\text{mm}$ and at 4050 r/min , that is, at a cutting condition that was otherwise globally unstable (see Figure 3). Measured displacements and active damping forces with a representative increment level of dK of 10 Ns/m for four different gain updating times are shown in Figure 6, and results for a fixed gain updating time of 25% of the DAQ time for four different levels of gain increments are shown in Figure 7. Results in Figures 6 and 7 are for the case of the initialized gain being zero.

Figures 6 and 7 show how the response and force both grow till the control action stabilizes the process. From Figure 6, for the fixed gain increment of $dK = 10$, it is evident that when the gain increment rate is 25% of the DAQ time, the system stabilizes quicker than slower gain updating rates. It is also interesting to note that the gain reaches its saturation set-point for increment rates being 25, 50, and 75% of the DAQ time; however, for the case of the gain updating rate equalling the DAQ rate, the gain stabilizes

at 190 Ns/m which is less than the saturation set-point. From Figure 7, it is also clear that the process takes longer to stabilize for smaller increments in the gain. Also, interestingly, for smaller gain increments, the gain stabilizes at values lower than higher gain increments. Though the process stabilizes quickest for when the gain increment in 200 Ns/m , that is, the maximum allowable, the measured active damping force shown in Figure 7(b) shows that, for this case, there is a sudden application of force. This impact force may damage the actuator, and hence, the use of this large gain increment is not recommended. Such systematic characterization that is possible on a HiL simulator can guide real experimentation on real machines.

Seeing that higher gain increments with shorter updating times result in the process being stabilized quicker, experiments for stabilizing cutting in the bistable region are conducted for a gain increment level of $dK = 10$ and with the gain updating time being 25% of the DAQ time. To check if adaptive tuning for interrupted turning is effective under perturbations, hammer blows were provided to the flexure for emulated cutting at point 'D' marked in Figure 8(a), that is, at an operating point that lies within the bistable region. The stability boundaries shown in

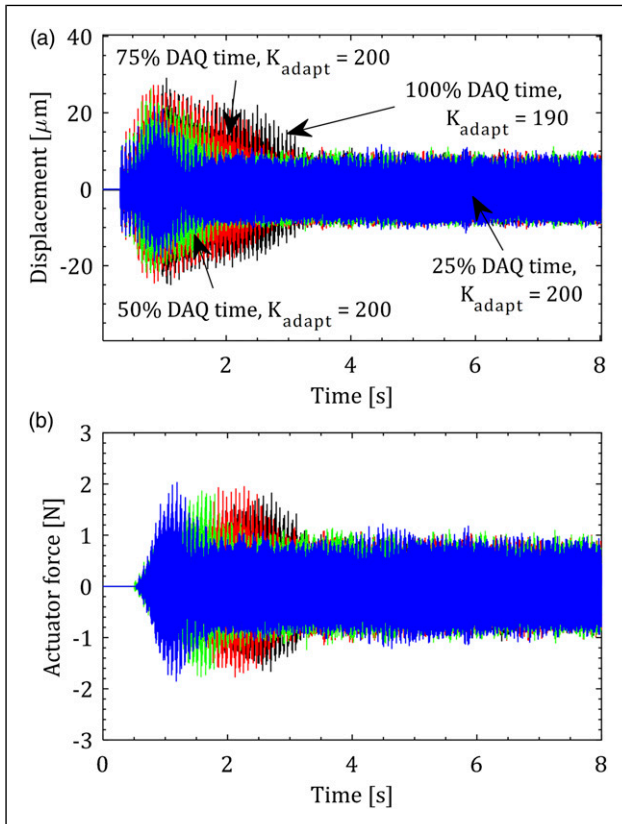


Figure 6. Results with $dK = 10\text{ Ns/m}$ and with different DAQ times for gain updating. (a) Measured displacement and (b) measured active damping force.

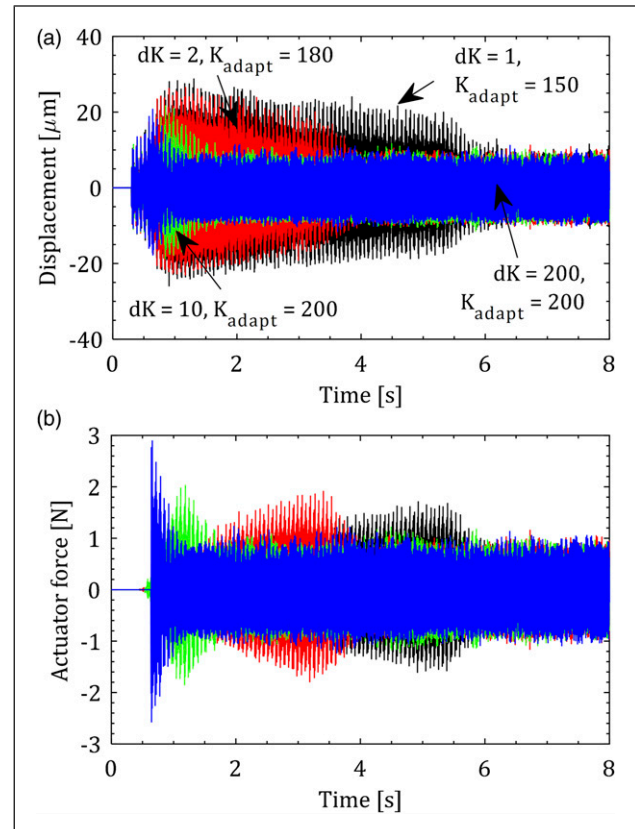


Figure 7. Results with different values of dK and with a fixed 25% of DAQ time for gain updating. (a) Measured displacement and (b) measured active damping force.

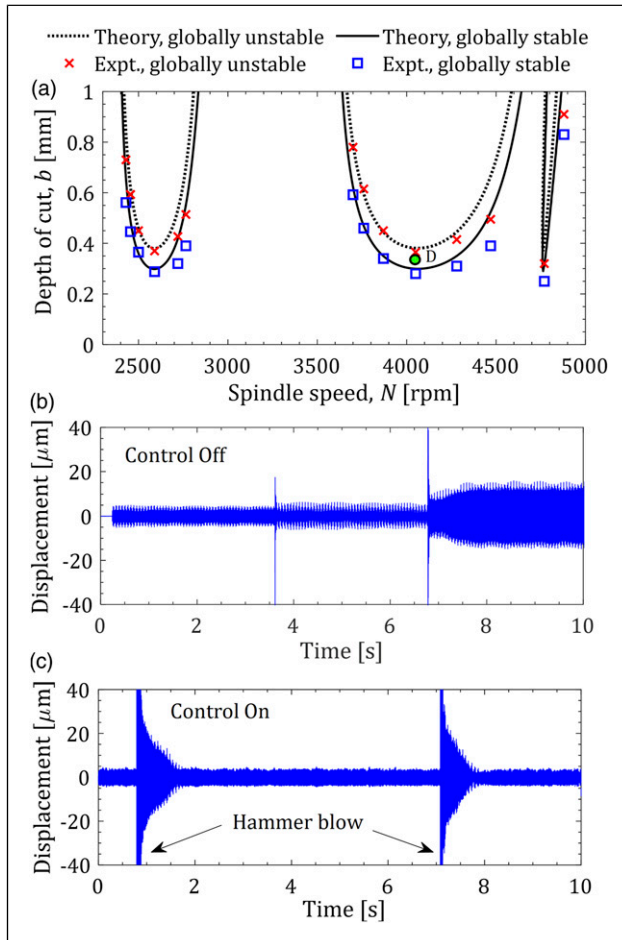


Figure 8. (a) Stability for interrupted turning; (b) response to perturbations for the control being ‘off’ for cutting at point ‘D’; and (c) response to perturbations with adaptive control for cutting at point ‘D’.

Figure 8(a) are the same as those shown in Figure 3. Results of without and with adaptive active damping are shown in Figure 8(b) and Figure 8(c), respectively.

For the case of the controller being ‘off’, from Figure 8(b), it is evident that the system is stable for small perturbations and is unstable for large ones. Whereas for the control being ‘on’, from Figure 8(c), it is also amply clear that the response stabilizes even after large perturbations with the use of an adaptive control scheme. Though results shown above are for a specific operating point lying within the bistable region, the proposed adaptive scheme may also be used to stabilize cutting for cutting conditions that lie in globally unstable regions for when the controller is ‘off’ – as has indeed already been demonstrated in the characterization experiments summarized in Figures 6 and 7. And, though the proposed adaptive control scheme has been used to successfully stabilize cutting in the bistable regimes, it may also be used to stabilize cutting in the presence of other

nonlinearities in machine tools. The use of this adaptive control scheme to detect and suppress chatter in near real-time during real cutting processes is part of our planned future follow-on research.

6. Conclusions

This paper has demonstrated through experimental emulations on a HiL simulator that for the case of highly interrupted turning processes with nonlinear force characteristics, bistabilities can co-occur with lobes and lenses. These findings validate earlier other reported theoretical observations. Since cutting in bistable regimes should be avoided, we demonstrated the use of active damping to stabilize cutting with interruptions/perturbations. We successfully implemented an adaptive gain tuning scheme that adapts the gain to the level of interruption/perturbation. To facilitate real-time detection of instabilities and their control, we characterized the efficacy of the gain updating scheme for its dependence on the time required to update the gain and for its dependence on the levels of gain increments and observed that higher gain increments with shorter updating times result in the process being stabilized quicker. We show that the simulator makes an excellent non-destructive platform for characterization of instabilities and for testing of active vibration schemes to mitigate them. Since circumventing instabilities in interrupted turning is an important technological problem, our results can help motivate mitigation strategies during real cutting on real machines, including the design and implementation of adaptive active damping control techniques.

Acknowledgments

The authors acknowledge Mr Pulkit Jain’s help in developing the software part of the HiL simulator and Mr Pankaj Deora for valuable discussions on adaptive control.



Declaration of conflicting interests

The author(s) declared no potential conflicts of interest with respect to the research, authorship, and/or publication of this article.

Funding

The author(s) disclosed receipt of the following financial support for the research, authorship, and/or publication of this article: This work was supported by the Government of India’s Impacting Research Innovation and Technology (IMPRINT) initiative through project number IMPRINT 5509.

ORCID iDs

Govind N. Sahu  <https://orcid.org/0000-0001-7722-4107>
 Mohit Law  <https://orcid.org/0000-0003-2659-4188>

References

- Abele E, Pfeiffer G, Jalizi B, et al. (2016) Simulation and development of an active damper with robust μ -control for a machine tool with a gantry portal. *Production Engineering* 10(4): 519–528.
- Bayly PV, Halley JE, Mann BP, et al. (2003) Stability of interrupted cutting by temporal finite element analysis. *Journal of Manufacturing Science and Engineering* 125(2): 220–225.
- Chen L, Zhang L and Man J (2015) Effect of nominal chip thickness on stability of interrupted turning. *Advances in Mechanical Engineering* 7(2): 579178.
- Chung B, Smith S and Tlusty J (1997) Active damping of structural modes in high-speed machine tools. *Journal of Vibration and Control* 3(3): 279–295.
- Claesson I and Håkansson L (1998) Adaptive active control of machine-tool vibration in a lathe. *International Journal of Acoustics and Vibration* 3(4): 155–162.
- Corpus WT and Endres WJ (2004) Added stability lobes in machining processes that exhibit periodic time variation, part 2: experimental validation. *Journal of Manufacturing Science and Engineering* 126(3): 475–480.
- Cowley A and Boyle A (1969) Active dampers for machine tools. *CIRP Annals* 18(2): 213–222.
- Davies MA, Pratt JR, Dutterer B, et al. (2002) Stability prediction for low radial immersion milling. *Journal of Manufacturing Science and Engineering* 124(2): 217–225.
- Dombovari Z, Wilson RE and Stepan G (2008) Estimates of the bistable region in metal cutting. *Proceedings of the Royal Society A: Mathematical, Physical and Engineering Sciences* 464(2100): 3255–3271.
- Fallah M and Moetakef-Imani B (2019) Adaptive inverse control of chatter vibrations in internal turning operations. *Mechanical Systems and Signal Processing* 129: 91–111.
- Ganguli A, Deraemaeker A, Horodincu M, et al. (2005) Active damping of chatter in machine tools-demonstration with a ‘hardware-in-the-loop’ simulator. *Proceedings of the Institution of Mechanical Engineers, Part I: Journal of Systems and Control Engineering* 219(5): 359–369.
- Ganguli A, Deraemaeker A, Romanescu I, et al. (2006) Simulation and active control of chatter in milling via a mechatronic simulator. *Journal of Vibration and Control* 12(8): 817–848.
- Inspurger T and Stépán G (2004) Updated semi-discretization method for periodic delay-differential equations with discrete delay. *International Journal for Numerical Methods in Engineering* 61(1): 117–141.
- Kalmar-Nagy T, Pratt JR, Davies MA, et al. (1999) Experimental and analytical investigation of the subcritical instability in metal cutting. In: Proceedings of DETC’99, 17th ASME Biennial Conference on Mechanical Vibration and Noise, Las Vegas, NV, USA, 12–15 September 1999, pp. 1721–1729. American Society of Mechanical Engineers.
- Kienzle O (1952) Die Bestimmung von Kräften und Leistungen an spanenden Werkzeugen und Werkzeugmaschinen. *VDI-Z* 94(11): 299–305.
- Kleinwort R, Platz J and Zaeh MF (2018) Adaptive active vibration control for machine tools with highly position-dependent dynamics. *International Journal of Automation Technology* 12(5): 631–641.
- Mancisidor I, Beudaert X, Etxebarria A, et al. (2015a) Hardware-in-the-loop simulator for stability study in orthogonal cutting. *Control Engineering Practice* 44: 31–44.
- Mancisidor I, Munoa J, Barcena R, et al. (2015b) Coupled model for simulating active inertial actuators in milling processes. *The International Journal of Advanced Manufacturing Technology* 77(1–4): 581–595.
- Molnar TG, Inspurger T and Stepan G (2019) Closed-form estimations of the bistable region in metal cutting via the method of averaging. *International Journal of Nonlinear Mechanics* 112: 49–56.
- Munoa J, Mancisidor I, Loix N, et al. (2013) Chatter suppression in ram type travelling column milling machines using a biaxial inertial actuator. *CIRP Annals* 62(1): 407–410.
- Sahu GN, Vashisht S, Wahi P, et al. (2020) Validation of a hardware-in-the-loop simulator for investigating and actively damping regenerative chatter in orthogonal cutting. *CIRP Journal of Manufacturing Science and Technology* 29: 115–129.
- Sahu GN, Jain P, Wahi P, et al. (2021) Emulating bistabilities in turning to devise gain tuning strategies to actively damp them using a hardware-in-the-loop simulator. *CIRP Journal of Manufacturing Science and Technology* 32: 120–131.
- Seguy S, Arnaud L and Inspurger T (2014) Chatter in interrupted turning with geometrical defects: an industrial case study. *The International Journal of Advanced Manufacturing Technology* 75(1–4): 45–56.
- Shi HM and Tobias SA (1984) Theory of finite amplitude machine tool instability. *International Journal of Machine Tool Design and Research* 24(1): 45–69.
- Stépán G, Inspurger T and Szalai R (2005) Delay, parametric excitation, and the nonlinear dynamics of cutting processes. *International Journal of Bifurcation and Chaos* 15(09): 2783–2798.
- Stepan G, Beri B, Miklos A, et al. (2019) On stability of emulated turning processes in HIL environment. *CIRP Annals* 68(1): 405–408.
- Szalai R and Stépán G (2006) Lobes and lenses in the stability chart of interrupted turning. ASME. *Journal of Computational and Nonlinear Dynamics* 1(3): 205–211.
- Tlusty J and Ismail F (1981) Basic non-linearity in machining chatter. *CIRP Annals* 30(1): 299–304.
- Urbikain G, De Lacalle LL and Fernández A (2014) Regenerative vibration avoidance due to tool tangential dynamics in interrupted turning operations. *Journal of Sound and Vibration* 333(17): 3996–4006.
- Zaeh MF, Kleinwort R, Fagerer P, et al. (2017) Automatic tuning of active vibration control systems using inertial actuators. *CIRP Annals* 66(1): 365–368.
- Zanka RM, Bachrathy D and Mészáros I (2010) Smoothed force model for interrupted high precision hard turning. In: 20th International GTE conference Manufacturing, Budapest Hungary, 20–21 October 2010, pp. 1–8.